



White matter microstructural differences identified using multi-shell diffusion imaging in six-year-old children born very preterm

Julia M. Young^{a,c,g,*}, Marlee M. Vandewouw^{a,c}, Sarah I. Mossad^{a,c,g}, Benjamin R. Morgan^{a,c}, Wayne Lee^a, Mary Lou Smith^{b,c,g}, John G. Sled^{d,e}, Margot J. Taylor^{a,c,f,g}

^a Diagnostic Imaging, Hospital for Sick Children, Toronto, ON, Canada

^b Department of Psychology, Hospital for Sick Children, Toronto, ON, Canada

^c Neurosciences and Mental Health, SickKids Research Institute, Toronto, ON, Canada

^d Translational Medicine, SickKids Research Institute, Toronto, ON, Canada

^e Department of Biomedical Physics, University of Toronto, Toronto, ON, Canada

^f Department of Medical Imaging, University of Toronto, Toronto, ON, Canada

^g Department of Psychology, University of Toronto, Toronto, ON, Canada

ARTICLE INFO

Keywords:

Preterm
Diffusion tensor imaging
White matter
Neurite density index
Orientation dispersion index
Cognition

ABSTRACT

Introduction: The underlying microstructural properties of white matter differences in children born very preterm (< 32 weeks gestational age) can be investigated in depth using multi-shell diffusion imaging. The present study compared white matter across the whole brain using diffusion tensor imaging (DTI) and neurite orientation dispersion and density imaging (NODDI) metrics in children born very preterm and full-term children at six years of age. We also investigated associations between white matter microstructure with early brain injury and developmental outcomes.

Method: Multi-shell diffusion imaging, T1-weighted anatomical MR images and developmental assessments were acquired in 23 children born very preterm (16 males; mean scan age: 6.57 ± 0.34 years) and 24 full-term controls (10 males, mean scan age: 6.62 ± 0.37 years). DTI metrics were obtained and neurite orientation dispersion index (ODI) and density index (NDI) were estimated using the NODDI diffusion model. FSL's tract-based spatial statistics were performed on traditional DTI metrics and NODDI metrics. Voxel-wise comparisons were performed to test between-group differences and within-group associations with developmental outcomes (intelligence and visual motor abilities) as well as early white matter injury and germinal matrix/intraventricular haemorrhage (GMH/IVH).

Results: In comparison to term-born children, the children born very preterm exhibited lower fractional anisotropy (FA) across many white matter regions as well as higher mean diffusivity (MD), radial diffusivity (RD), and ODI. Within-group analyses of the children born very preterm revealed associations between higher FA and NDI with higher IQ and VMI. Lower ODI was found within the corona radiata in those with a history of white matter injury. Within the full-term group, associations were found between higher NDI and ODI with lower IQ.

Conclusion: Children born very preterm exhibit lower FA and higher ODI than full-term children. NODDI metrics provide more biologically specific information beyond DTI metrics as well as additional information of the impact of prematurity and white matter microstructure on cognitive outcomes at six years of age.

1. Introduction

Very preterm birth (< 32 weeks gestational age) can disrupt sensitive processes of fibre organization and myelination (Kinney et al.,

1988). Additional factors experienced by children born very preterm such as illness, brain injury, and ex-utero environments can impact white matter maturation and its supportive role in cognition (Dubois et al., 2008). Children born very preterm are at greater risk for

Abbreviations: DTI, diffusion tensor imaging; NODDI, neurite orientation dispersion and density imaging; ODI, orientation dispersion index; ND, neurite density index; FA, fractional anisotropy; MD, mean diffusivity; AD, axial diffusivity; RD, radial diffusivity; GMH/IVH, germinal matrix/intraventricular haemorrhage; MRI, magnetic resonance imaging; IQ, intelligence quotient; VMI, visual motor integration; VP, visual perception; MC, motor coordination; VPT, very preterm; FT, full-term

* Corresponding author at: 555 University Avenue, Toronto, Ontario M5G 1X8, Canada.

E-mail address: julia.young@mail.utoronto.ca (J.M. Young).

<https://doi.org/10.1016/j.nicl.2019.101855>

Received 3 August 2018; Received in revised form 8 April 2019; Accepted 2 May 2019

Available online 04 May 2019

2213-1582/© 2019 The Authors. Published by Elsevier Inc. This is an open access article under the CC BY-NC-ND license

(<http://creativecommons.org/licenses/by-nc-nd/4.0/>).

neurodevelopmental impairments in cognitive abilities, behaviour, and social/emotional functioning but underlying contributions from white matter microstructure are not well understood (Mangin et al., 2017; Woodward et al., 2009). Therefore, understanding the characteristics of fibre organization and myelination of white matter in children born very preterm is necessary for elucidating developmental disturbances in these children.

Diffusion tensor imaging (DTI) and its indices of fractional anisotropy (FA), mean diffusivity (MD), axial diffusivity (AD) and radial diffusivity (RD) are commonly studied to evaluate white matter structures. While providing insight into the microstructural properties of white matter, DTI metrics are also sensitive in detecting group differences and age-related changes. However, they lack specificity in terms of what particular properties may be contributing to group differences. Changes and reductions in FA across development can be driven by multiple contributing factors such as myelination, organization of axons, membrane permeability, axon density, partial volume effects, axon size and the number of axons (Jones et al., 2013). Diffusion imaging with multiple b-values, including higher b-values and number of gradient directions, provides an opportunity to measure more specific information regarding the microstructure of white matter that can overcome some of the ambiguities of DTI metrics. One such method is the biophysical model, neurite orientation dispersion and density imaging (NODDI) (Zhang et al., 2012), which quantifies structural properties of axons and dendrites (neurites) that FA is unable to infer. The NODDI model differentiates three tissue types: intra-cellular, extra-cellular, and CSF compartments (Zhang et al., 2012). Two primary indices, orientation dispersion (ODI), and neurite density index (NDI), are estimated with this method. ODI represents the angular variation of neurite orientations, reflecting the bending and fanning of axons and areas of crossing fibres (Zhang et al., 2012). NDI represents the intra-cellular volume fraction, estimating the density of axons within a voxel (Zhang et al., 2012).

Only a few studies have used multi-shell diffusion imaging with DTI and NODDI metrics to identify early brain maturation and its variability across different tissues. Before term-equivalent age, brain development is dominated by increases in FA and NDI, particularly in white matter connections between deep grey matter and central cortical regions (Batalle et al., 2017). Following very preterm birth until term-equivalent age, age-related changes of ODI and NDI in grey matter were identified (Eaton-rosen et al., 2015). During this time, the cortex and thalamus demonstrated lower and higher FA values, respectively, yet with different contributions of ODI and NDI. Higher FA values within the thalamus were contributed by higher values of NDI, reflecting active myelinating processes (Eaton-rosen et al., 2015). Higher FA values within the cortex were contributed by lower ODI values, reflecting microstructural complexity although the NODDI metrics do not completely explain the changes occurring within these tissues (Eaton-rosen et al., 2015; Melbourne et al., 2016). At term-equivalent and one month of age, ODI and NDI were also shown to vary across white matter regions concordant with different microstructural properties, different developmental timing of white matter regions, and regional asymmetries (Dean et al., 2017; Kunz et al., 2014). For instance, the corpus callosum and internal capsules exhibited the lowest axonal ODI, reflecting their highly-organized axons, early developmental trajectory and high FA relative to other tracts (Dean et al., 2017; Kunz et al., 2014; Young et al., 2017). In contrast, tracts that were more peripheral in the brain had higher ODI values, reflecting less mature white matter and potentially greater branching of axons in those areas (Dean et al., 2017).

Developmental changes in diffusion tensor and NODDI measures are not uniform across brain regions. Cross-sectional studies from childhood to adolescence indicate that NDI demonstrates stronger age-related changes compared to FA and diffusivity (MD, AD, RD) in both white matter and subcortical grey matter (Genc et al., 2017; Mah et al., 2017). These studies suggest that axonal packing is strongly associated

with early brain development. Concurrently, FA was found to be more highly correlated to ODI, despite ODI having weak associations with age in childhood to early adolescence (Mah et al., 2017). Rapid increases in NDI occur primarily in childhood, but then slow down throughout adulthood (Chang et al., 2015). This developmental trajectory differs from ODI, which increases more slowly in childhood and then more rapidly in adulthood (Chang et al., 2015).

A recent study by Kelly et al. (2016) identified white matter differences using DTI and NODDI metrics in a large retrospective sample of children born very preterm at seven years of age. Lower FA values were identified in a small cluster within the right hemisphere overlapping the cingulum, inferior longitudinal fasciculus, inferior frontal-occipital fasciculus, uncinate fasciculus, anterior thalamic radiation, and external capsule. In contrast, extensive differences of axon orientation dispersion were identified in about one fifth of the total white matter examined, including areas where FA differences were found. Moreover, the authors identified associations between FA, ODI, and NDI with neurodevelopmental outcomes such as IQ, motor abilities, academics, and behavioural measures in the children born very preterm. FA and neurite density index were positively correlated with IQ, demonstrating one of the first studies to relate NODDI measures to cognitive abilities in childhood.

In this prospective study, we assessed the development of commonly investigated white matter tracts in six-year-old children born very preterm. Previously at four years of age, reduced FA within many white matter tracts were found in an overlapping sample compared to full-term matched controls (Young et al., 2018). Associations between FA and IQ were also found at four years in the full-term children but not the children born very preterm (Young et al., 2018). In the present study, our first objective was to identify whether these FA differences were sustained two years later using multi-shell diffusion imaging. Our second objective was to calculate NODDI measures of ODI and NDI to delineate additional microstructural white matter differences and their potential contributions to FA differences found between very preterm and full-term children. In addition, relations between DTI and NODDI measures with developmental outcomes were examined in each group. In the children born very preterm, we also investigated relations between the DTI and NODDI measures with prematurity and early brain injury such as white matter injury and germinal matrix/intraventricular haemorrhage. We hypothesized that the measures of ODI and NDI would also be sensitive to differences that were expected to be found with FA. For instance, we expected that the children born very preterm would have higher ODI and lower NDI within white matter regions compared to full-term children as well as in relation to early brain injury. Furthermore, we also expected that higher ODI and lower NDI would be associated with lower scores of IQ and visual-motor ability.

2. Methods

2.1. Participants

Seventy-three children were recruited for this study. Of those, thirty-nine children were born very preterm (< 32 weeks GA) and recruited as a part of an ongoing larger longitudinal study, conducted between 2009 and 2017 at the Hospital for Sick Children in Toronto, Canada. Exclusion criteria for the children born very preterm included those with any known chromosomal or major congenital abnormalities. Thirty-four full-term children (> 37 weeks GA) were also recruited. Exclusion criteria for full-term children included prematurity, learning, language, neurological or developmental disabilities, non-English speakers, as well as magnetic resonance imaging (MRI) incompatibility based on a screening interview. An informed consent to the study was signed by parents and informed assent was provided by the children. The research ethics board at the Hospital for Sick Children approved the study protocol.

Table 1
Clinical and radiological characteristics at VPT birth.

Characteristic	Mean (SD) or number (%)
Gestational Age (weeks)	28.8 (1.4)
Males	16 (69.6)
Birth Weight (g)	1161.6 (233.4)
Head circumference (cm)	25.5 (1.9)
Intrauterine growth restriction	3 (13.0)
Caesarean-section delivery	17 (73.9)
Multiple births	5 (21.7)
Apgar score at 5 min	7.3 (1.7)
CRIB II	7.1 (2.3)
Endotracheal tube days	11.5 (15.5)
Oxygen administration days	15.2 (22)
Positive pressure ventilation	13.4 (10.8)
Patent ductus arteriosus (treated)	6 (26.1)
Sepsis (cultures positive)	9 (39.1)
Premature Rupture of Membranes	2 (8.7)
Necrotizing enterocolitis (stage 2 & 3)	3 (13.0)
Bronchopulmonary dysplasia	4 (17.4)
GMH (Grade 1–2)	4 (17.4)
GMH (Grade 3–4)	5 (21.7)
White Matter lesions	8 (34.8)

CRIB II - Clinical Risk index for Babies; GMH - Germinal Matrix Haemorrhage.

2.2. Perinatal clinical and radiological measures

Perinatal clinical information was obtained for the children born very preterm during their stay in the neonatal intensive care unit. Information such as demographics, significant events during pregnancy, and medical interventions are summarized in Table 1. Paediatric neuroradiologists and neurologists assessed each of the structural T1- and T2- weighted images for the children born very preterm shortly following birth. The presence of white matter injury and germinal matrix/intraventricular haemorrhage (GMH/IVH) was identified. White matter injury was identified as mild to moderate (T1 signal abnormalities in three or fewer areas), and severe (T1 signal abnormalities in > 5% of hemisphere) levels of injury (Miller et al., 2003). The grade of GMH/IVH was determined according to the classification by Papile and Volpe for cranial ultrasonography findings adapted to MRI (Papile et al., 1978; Volpe, 2008). At six years of age, paediatric neuroradiologists also assessed each of the children's structural T1-, T2-weighted and FLAIR images. Any incidental findings were noted.

2.3. Developmental assessments and maternal education

Developmental assessments were completed for the children born very preterm who returned for follow-up as well as the recruited full-term children. For each assessment, raw scores were converted into standardized scores with a population mean of 100 (50th percentile of typical development) and a standard deviation of 15. Intelligence quotients (IQ) were determined by the 2-subtest Wechsler Abbreviated Scale of Intelligence (WASI; Wechsler, 1999) using Canadian norms, which included the vocabulary and matrix reasoning subtests to estimate general intellectual ability. Visual-motor integration (VMI) and supplemental tests of visual perception (VP) and motor coordination (MC) were assessed by the Beery-Buktenica Test of Visual Motor Integration (Beery et al., 2010). Measures of VP and MC were not obtained for one full-term child.

Levels of maternal education were obtained for all the children. Percentages of mothers with high school or college education, university education and post-graduate education are reported.

2.4. MRI data acquisition

MRI scans were acquired with a 3T Siemens Trio scanner and 12 channel head coil. Three separate diffusion datasets were acquired

along 60 directions (SE-EPI, b-values = 700/1000/2850 s/mm²; repetition time: 10700/8800/10700 ms; echo time: 115/87/115 ms; field of view: 244 × 244 × 140mm; resolution: 2 mm isotropic; total scan time: 40.9 min) were obtained with 26 interleaved b = 0 s/mm² volumes. Anatomical T1-weighted (MPRAGE) images (repetition/echo time: 2300/2.96 ms; field of view: 192 × 240 × 256 mm; resolution: 1 mm isotropic; scan time: 5 min) were obtained. All of the scans were collected when the children were awake and watching a movie. Images were inspected for gross motion artefacts and anatomical abnormalities. We obtained 32 T1-weighted images and diffusion data in the children born very preterm, and 24 of the children had complete multi-shell scans. One child born very preterm had ventriculomegaly and was excluded from analyses. A total of 30 T1-weighted and diffusion data were obtained in the full-term children, and 24 of the children had complete multi-shell diffusion scans.

2.5. Diffusion processing

FSL tools (Jenkinson et al., 2012) and custom scripts were used to correct for eddy current distortions and head motion. The mean for each b-value (0, 700, 1000, 2850 s/mm²) was calculated, and transformations between the mean b = 0 image and each mean b-value were obtained using FSL's FLIRT (Jenkinson et al., 2002). Each individual volume was first registered to its corresponding mean image, and then to the mean b = 0 image by applying the previous transformation, while adjusting corresponding b-vectors. Following visual inspection, all volumes for each child were included due the large number of volumes acquired and the small number of motion corrupted volumes across subjects. The average percentage of motion corrupted volumes in the b = 1000 s/mm² shell was 2.08% (range: 0–15%). The average percentage of motion corrupted volumes in all shell together was 5.29% (range: 0–28.3%).

DTI metrics (FA, AD, MD, RD) were calculated and extracted from the output of the RESTORE algorithm using the b = 1000 s/mm² shell (Chang et al., 2005). NODDI measures of orientation dispersion index (ODI) and neurite density index (NDI) were estimated using all three b-values with the NODDI Matlab toolbox version 1.0 (Zhang et al., 2012). To account for the differences in TR and TE across the three shells, the volumes in each shell were normalized with their respective mean b = 0 image, as per the developer's recommendation (Counsell et al., 2014).

2.6. Tract-based spatial statistics (TBSS)

Analyses of the DTI (FA, AD, MD, RD) and NODDI metrics (ODI, NDI) were conducted using FSL's TBSS method (Smith et al., 2006). Nonlinear co-registration of all the children's fractional anisotropy (FA) images was performed between every child. One image that was the most representative of the group was used as the target image and then registered to MNI151 standard space. Therefore, each FA image underwent a combined nonlinear registration and linear registration to the target image. A mean of all the FA images and a skeleton representing the centre of major white matter tracts within the brain was generated and thresholded at 0.2. All of the same registrations were applied to each child's MD, AD, RD, ODI, and NDI data. Lastly, the diffusion data were projected onto the skeleton.

3. Statistical analysis

3.1. Participant characteristics

Between the children born very preterm and full-term children, sample differences of male and female sex ratios as well as age at scan were tested using a chi-square and two-tailed *t*-test. Group differences in developmental test scores were also tested using two-tailed *t*-tests. To compare the three maternal education levels (high school or college

education, university education, and post-graduate education) between groups, a non-parametric Mann-Whitney *U* Test was employed. Moreover, the relation between the three levels of maternal education and developmental test scores were examined using a one-way ANOVA tests for each group separately. The significance threshold was set to $p \leq .05$.

3.2. TBSS analyses

Between and within-group voxel-wise analyses were performed with FSL Randomise (Anderson and Robinson, 2001) using 5000 permutations and threshold-free cluster enhancement (Smith and Nichols, 2009). Significance was defined as $p < .05$ following corrections for multiple comparisons. Between group analyses were conducted using a general linear model with group, age at scan and sex as explanatory variables. Interaction analyses were also performed between groups with outcome measures (IQ and VMI). This was performed for all DTI metrics (FA, AD, MD and RD) as well as the NODDI metrics (ODI and NDI). Within the preterm group, additional voxel-wise regression analyses were performed between all of the DTI and NODDI metrics with GA, presence of white matter injury, presence of GMH/IVH, and developmental measures (IQ and VMI). Within the full-term group, voxel-wise regression analyses were performed between all of the DTI and NODDI metrics and developmental measures (IQ and VMI). All significant voxels of the white matter skeleton were thickened to help visualize the results.

To plot and visualize the data extracted from significant within-group TBSS analyses by white matter regions, the JHU DTI-based labelled atlas (Mori et al., 2005) was registered to MNI space and applied to the thresholded FA skeleton for significant TBSS analyses of interest. The thresholded FA skeleton was applied to both the children born very preterm and full-term. Average DTI and NODDI values were estimated within each white matter region. Scatter plots depict the associations of the DTI and NODDI values and neurodevelopmental outcome measures.

4. Results

4.1. Participant characteristics

Twenty-three children born very preterm (16 males, 7 females; mean scan age: 6.57 ± 0.34 years; mean gestational age: 28.8 ± 1.4 weeks) were included with useable multi-shell diffusion data and developmental assessments. Perinatal clinical and radiological characteristics for the children born very preterm are provided in Table 1. Eight (34.8%) children born very preterm had incidences of white matter lesions (six mild/moderate injury and two severe injury) and nine (39.1%) had incidences of GMH/IVH of any severity on structural scans following birth. Twenty-four full-term children (10 males, 14 females; mean age: 6.62 ± 0.37 years) had useable multi-shell diffusion data and developmental assessments. No sex differences were found between the group samples ($X^2(1) = 3.69$, $p = .054$). There was also no difference in age at scan between groups ($p = .697$).

The education levels of the mothers of the children born very preterm were 26.1% high school or college, 60.7% university, and 13% post-graduate. The education levels of the mothers of the full-term children were 21.7% high school or college, 56.5% university, and 21.7% post-graduate. There were no differences in education levels between groups ($p = .645$).

Performance on the neurodevelopmental tests was consistently lower for the children born very preterm than for the full-term children as shown in Table 2 and Supplemental Table 1. Compared to the general population, the mean of each measure (IQ, VMI, VP and MC) by group was in the average range apart from MC in the very preterm group, which was in the low average range. In the full-term group, developmental measures were not associated with maternal education levels (all $p > .05$). In the very preterm group, IQ, VMI and VP were

Table 2
Neurodevelopmental Measures and ANOVA Results.

	IQ	VMI	VP	MC
VPT	103.04 (11.75)	96 (8.5)	87.17 (13.58)	99.23 (16.77)
Full-term	112.36 (13.43)	102.13 (9.31)	95.08 (10.70)	107.17 (13.5)
df	45	45	44	44
T-statistic	-2.53	-2.349	-1.917	-2.158
p-value	0.015	0.023	0.036	0.062

not associated with maternal education levels (all $p > .05$); measures of MC were significantly different between maternal education levels in the children born very preterm ($p = .017$). The children born very preterm with mothers who had post-graduate training had significantly higher MC abilities than both those who had university training ($p = .017$) and high-school or college level training ($p = .0277$).

4.2. TBSS between-group analyses

Group differences were present between the children born very preterm and full-term children in FA, MD, RD and ODI metrics at $p < .05$ following multiple comparisons. Full-term children displayed significantly higher FA values than the children born very preterm within many white matter subregions across the white matter skeleton as shown in Fig. 1A. Regions of significance included the corpus callosum, anterior and posterior limb of the internal capsule, corona radiata (anterior, posterior, and superior), external capsule, posterior thalamic radiation, and cingulum among others. Supplemental Table 2 provides the subregions corresponding to the JHU white matter atlas where group differences were found as well as the number of significant voxels per region. Between-group differences were also found where the children born very preterm had significantly higher MD and RD values than the full-term children (Supplemental Table 2 and Supplemental Fig. 2). The children born very preterm had significantly higher ODI than the full-term children (Fig. 1B) in regions including the corpus callosum (genu, body, and splenium), corona radiata (anterior, superior, and posterior) and left anterior limb of the internal capsule and external capsule.

In addition, significant effects of age at scan were associated with MD, RD and NDI. Increasing MD and RD were associated with decreasing scan age and increasing NDI had a strong, widespread association with increasing scan age (all $p \leq .05$). The interaction analyses between the DTI and NODDI metrics and neurodevelopmental outcome measures (IQ and VMI) also revealed significant results. The slope of the association between FA and IQ was significantly greater in the children born very preterm than the full-term children ($p \leq .05$; Supplemental Fig. 3). The slope of the associations between AD, MD, and RD with IQ was significantly greater in the full-term children than the children born very preterm ($p \leq .05$). Furthermore, the slope of the associations between FA, AD, MD, RD, NDI, and ODI with VMI was significantly greater in the full-term children than the children born very preterm ($p \leq .05$).

4.3. TBSS within-group analyses in VPT group

In the children born very preterm, there were many areas of white matter with significant associations between DTI metrics and IQ. Similarly, there were many areas of white matter with significant associations between NODDI metrics and IQ. Significant associations were present between higher FA and NDI with higher scores of IQ (see Fig. 2A–B). In addition, significant associations were found between higher AD, MD, and RD with lower scores of IQ ($p < .05$) (Supplemental Table 2). Moreover, significant associations were found between higher AD, MD, and RD with lower scores of VMI as well as higher NDI and higher scores of VMI (all $p \leq .05$) (Supplemental Table 2 and Fig. 4). No associations were found between DTI and NODDI metrics

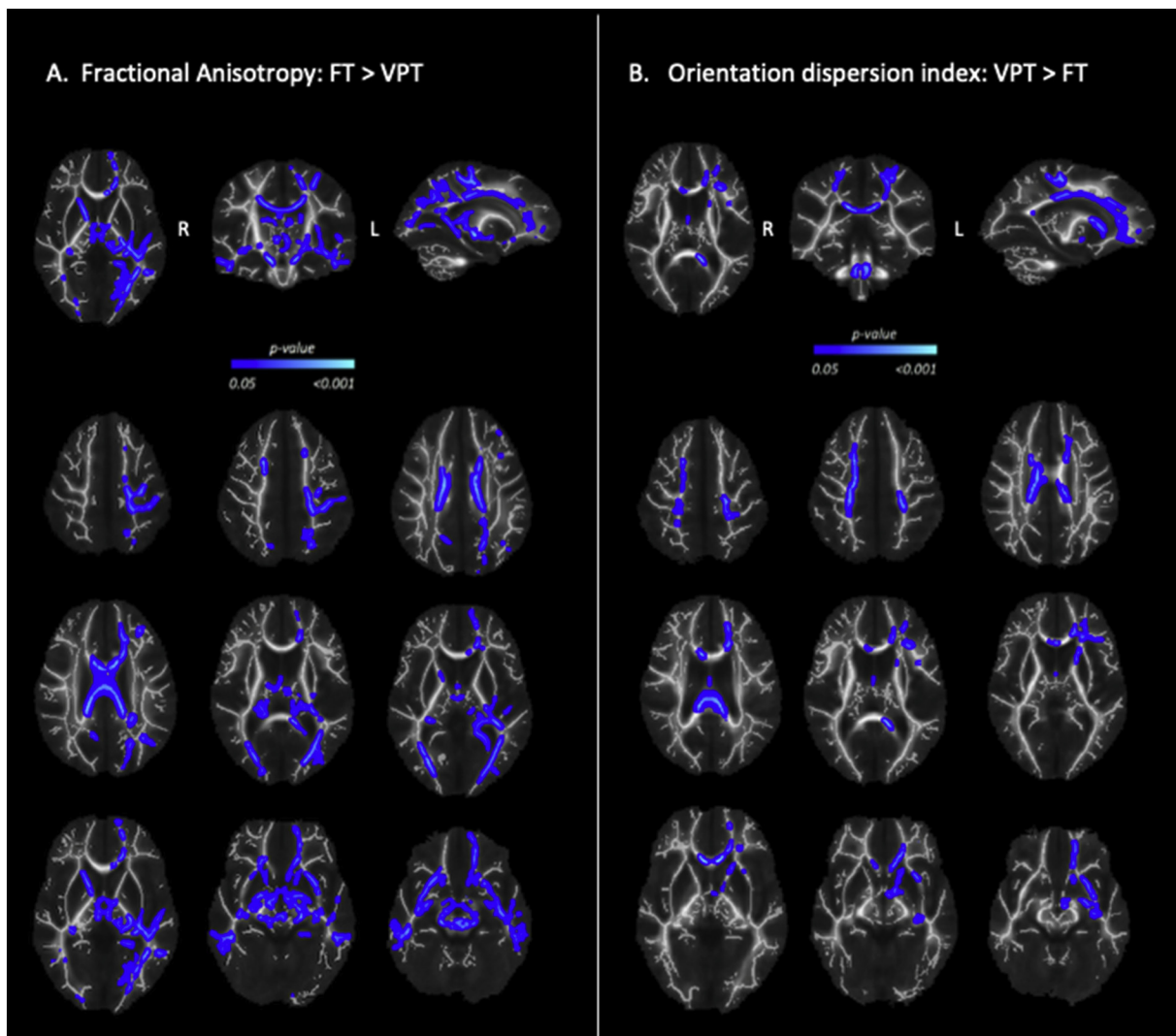


Fig. 1. FA and ODI between group results. A. TBSS analyses of group differences revealed reduced FA in the children born very preterm compared to the full-term children along the white matter skeleton ($p < .05$). Significant voxels are depicted in blue. Colour bars indicate p-values. B. Voxels with significantly higher neurite orientation dispersion in the children born very preterm are indicated in blue along the white matter skeleton.

with gestational age.

4.4. TBSS within group analyses in FT group

In the full-term children, many areas of white matter also showed associations between NODDI metrics and IQ. Higher NDI and ODI were associated with lower scores of IQ ($p < .05$) as shown in Fig. 2B and C. Subregions with significant voxels in the full-term group included the corpus callosum, corona radiata (anterior, superior, and posterior), posterior thalamic radiation, superior longitudinal fasciculus, and the anterior and posterior limb of the internal capsule. Supplemental Table 3 provides a full list of the subregions.

4.5. TBSS within group analyses with early brain injury

With respect to early brain injury, children born very preterm who had white matter injury identified following birth displayed lower ODI within the right superior corona radiata ($p \leq .05$) (see Fig. 3). No associations were found between the DTI and NODDI metrics and GMH/IVH.

5. Discussion

In children born very preterm, development of white matter differs from full-term children on a microstructural level. Examining these differences using NODDI opens a new perspective into the microstructural components that comprise white matter by quantifying two additional metrics from the traditional diffusion tensor model: ODI and NDI. We identified widespread reductions of FA as well as increases in MD, RD, and ODI in children born very preterm compared to term-born children at six years of age. In the children born very preterm, DTI and NODDI metrics were also associated with intellectual ability, visuo-motor skills and early white matter injury identified within the perinatal period. In the full-term children, additional associations between NODDI metrics and intellectual abilities were found. These alterations in microstructural properties of white matter that are present in childhood may help explain the origins of developmental differences as well as adverse functional outcomes.

Developmental studies using multi-shell diffusion imaging in young children are sparse and challenging due to long acquisition times. The few existing studies that applied NODDI to developmental populations have shown utility in understanding early brain development (Tamnes et al., 2017). NDI has been shown to have a stronger relationship with age than diffusion tensor metrics (FA, AD, MD, RD), thereby an

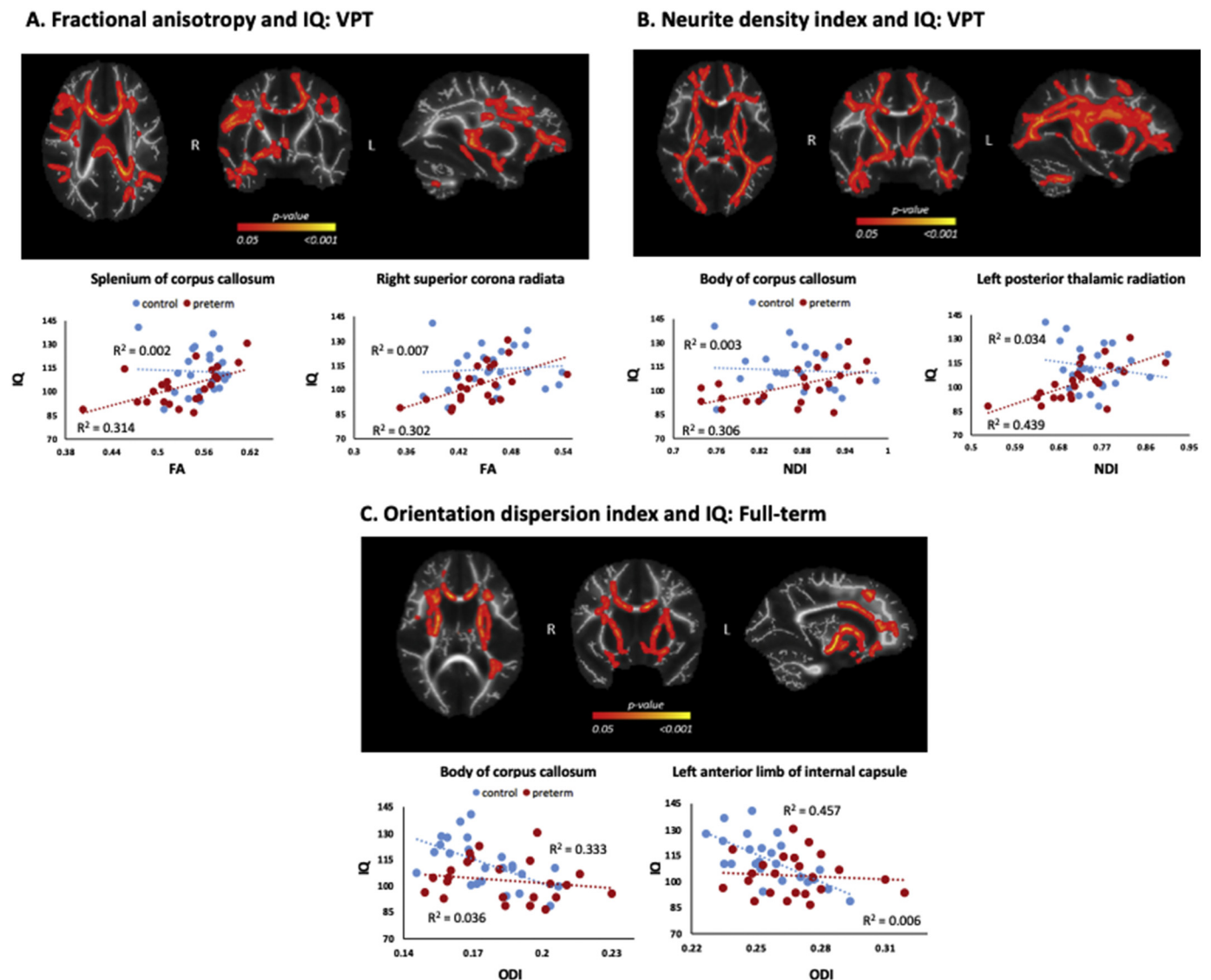


Fig. 2. Within-group results with outcomes. A. Within-group TBSS analyses of the children born very preterm demonstrated significant associations between increasing FA and higher scores of IQ as indicated by the white matter regions highlighted in red and yellow along the white matter skeleton ($p \leq .05$). Colour bars indicate p-values. The scatter plots below the TBSS results indicate data extracted from regions where there were significant findings from the within-group TBSS analyses of the children born very preterm; data from the full-term children are shown in blue and preterms are shown in red. B. Significant associations were found between increasing NDI and higher scores of IQ in the children born very preterm ($p \leq .05$). C. Significant associations were found between decreasing ODI and lower scores IQ in the full-term children ($p \leq .05$).

important contributor to increases of FA during childhood within white matter; however, ODI is more strongly correlated with FA irrespective of age (Chang et al., 2015; Genc et al., 2017; Tamnes et al., 2017; Zhang et al., 2012). Our study is one of the first prospective studies in six-year-old children born very preterm applying NODDI to multi-shell diffusion data. We found widespread reductions of FA as well as higher RD and MD in the children born very preterm compared to full-term children at the beginning of school-age, which were consistent with previous findings in an overlapping cohort of children at four years of age as well as an independent cohort of seven to nine-year-old very preterm children (Duerden et al., 2013; Young et al., 2018). The reductions in FA suggest that there may be a sustained maturational lag of white matter development as well as possible differences in the structural architecture of white matter in the children born very preterm. Moreover, increases in RD may indicate delayed maturation specific to myelination (Jones et al., 2013).

Higher ODI was identified within several white matter regions in the children born very preterm. The regions identified included the corpus

callosum (genu, body and splenium), corona radiata (anterior, superior, and posterior aspects), left external capsule, uncinata fasciculus, and anterior limb of the internal capsule. Most of the significant voxels were identified in the body of the corpus callosum and the left-sided corona radiata. The corpus callosum is a coherent fibre pathway, containing fibres that have consistent directionality along its macroscopic curvature (Budde and Annese, 2013). However, it also exhibits microscopic regional variations in orientation in its medial and lateral aspects (Budde and Annese, 2013). Low ODI in the corpus callosum has been found during the neonatal period in typically developing neonates, reflecting the very early organization of this fibre pathway (Dean et al., 2017). It is thought that the higher ODI, indicating greater bending and fanning of axons, in children born very preterm later in childhood may be a product of early disruptions to the organization of its characteristic densely packed parallel fibres prior to or during the neonatal period (Nossin-Manor et al., 2013; Young et al., 2017).

The corona radiata comprises projection fibres that extend towards the cortex from the internal capsule in subcortical regions. These fibres

Orientation dispersion index and white matter injury: VPT

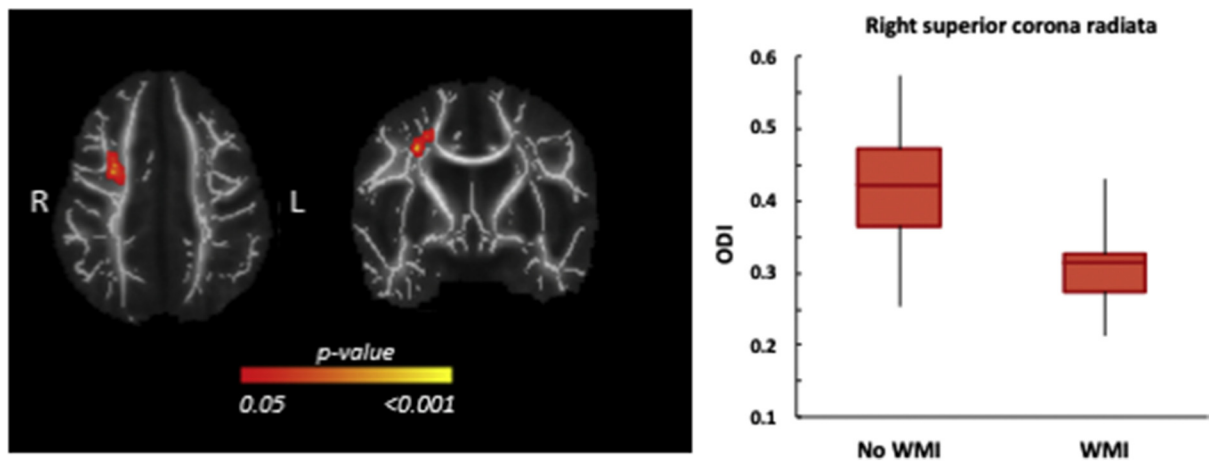


Fig. 3. Results with early brain injury. TBSS analyses revealed lower neurite orientation dispersion with early white matter injury in the children born very preterm within the right superior corona radiata ($p \leq .05$). The boxplot depicts the distribution of data between those with and without early white matter injury.

contain thalamic and motor projections involved in sensory and motor function (Catani et al., 2002). In late childhood and early adolescence, motor fibres within the internal capsule and cortical spinal tract have lower ODI values compared to other fibre regions, also reflecting early organization in concordance to that seen in the corpus callosum (Mah et al., 2017). Greater dispersion within the corona radiata in the children born very preterm highlights additional vulnerabilities of highly organized white matter structures. It is possible that differences in orientation dispersion are more pronounced in these structures as they are likely to be more coherent and less variable in their composition between individuals. Differences found in these areas support primary disruptions to thalamocortical fibres in early maturation, which are particularly vulnerable during the preterm period when axonal ingrowth via programmed migration paths outspread to designated regions of the cortical plate (Kostović and Judas, 2002). These deviances can impact secondary organization and further influence susceptibility to adversity with age (Dean et al., 2017; Rae et al., 2017).

Our findings of higher ODI coupled with lower FA in regions such as the corpus callosum and corona radiata have also been identified in other studies of infants and children (Dean et al., 2017; Eaton-Rosen et al., 2015; Genc et al., 2018; Kunz et al., 2014). As DTI metrics such as FA lack biological specificity, using NODDI metrics is advantageous over DTI metrics for specific interpretations of the organizational attributes of these structures. Axons within white matter tracts are understood to not always follow linear paths, which is better understood by NODDI measures such as ODI (Genc et al., 2018; Nilsson et al., 2012). Due to the redundancy between FA and ODI findings in the current study, it is reasonable to suggest that lower FA is partially contributed by axon dispersion. In the context of comparing children born very preterm to full-term children, the combination of higher ODI and lower FA is indicative of less organization within these regions and may characterize a potential developmental delay in white matter maturation during early childhood.

The effect of early brain injury was also explored within the group of children born very preterm. Lower ODI (in the absence of DTI findings) was found in relation to those who had white matter injury detected on MRI within two weeks of birth. This finding was specific to the superior corona radiata in the right hemisphere, consistent with the location of the majority of identified white matter lesions. A histological study of demyelinating white matter lesions from multiple sclerosis spinal cord pathology quantified NODDI metrics and found reduced variability in axonal orientations within the lesions, indicating reduced neurite complexity (Grussu et al., 2017). As reduced

orientation dispersion was indicative of pathology in the context of focal demyelination, early white matter injury in the children born very preterm may have a similar effect on the neural architecture of axons with respect to reducing the angular variation of the internal capsule and corona radiata pathways involved in sensorimotor processing. In addition, alterations of white matter microstructure identified early in development due to punctate white matter lesions may result in less complex white matter tracts later in childhood (Tusor et al., 2017). Taken together, the potential impact of ODI differences on white matter maturation should be interpreted in the context of the analysis as well as the white matter regions involved.

In the children born very preterm, intelligence was associated with NDI rather than ODI at six years of age. More specifically, positive associations were present between FA and NDI with intelligence and visuospatial skills. In addition, negative associations between MD, AD, and RD were found with intelligence and visuospatial skills. These findings indicate that white matter microstructure can help provide contributing explanatory factors for which children are slower to develop with their cognitive skills. NDI estimates the density of axons as well as the caliber of myelinated axons (Carper et al., 2017). Thus, reduced NDI can be consistent with abnormal myelin as well as neuronal loss, with overlapping microstructural contributions to RD (Timmers et al., 2016). Lower scores of intellectual abilities and visuospatial skills in the children born very preterm may be closely related to myelination.

In contrast, the full-term children exhibited differing relations with outcomes than the children born very preterm, demonstrating increasing NODDI metrics with lower scores of intellectual abilities. Higher NDI was unexpectedly associated with lower intellectual abilities, which may represent an effect of ongoing axonal pruning. It may also be possible that there is an optimal range of axonal density that benefits full-term children, reflected by relatively higher IQ. In addition, higher ODI was associated with lower scores of intellectual abilities in regions including the corpus callosum, internal capsules, external capsule, corona radiata and superior longitudinal fasciculus. Based on the strong association between ODI and IQ, full-term children may have increased sensitivity to microstructural deviances in axonal organization that involve highly organized white matter structures like the corpus callosum (Fig. 2C). Overall, the different associations with outcomes between the two groups may be due to different developmental processes contributing to cognitive abilities.

A recent study by Kelly et al. (2016) also investigated DTI and NODDI metrics using tract-based spatial statistics in a sample of seven-

year-old children born very preterm. Parallel findings between our prospective study and their retrospective study are promising for enhancing our understanding of white matter microstructural differences between children born very preterm and full-term children at early school-age. Results of their study indicated small areas of reduced FA and large areas (about 25%) of higher ODI within white matter in the very preterm born group (Kelly et al., 2016). While our results indicated more group differences with FA than ODI, neither study found group-level differences in NDI, suggesting that the angular variation of axons is an integral contributor to FA differences in this population. Similar to our study, they found that FA and NDI positively correlated with IQ in the very preterm group while they did not find significant correlations in the full-term group. These discrepancies are likely attributed to differences in sample characteristics such as age, sample size, and gestational age as well as differences in imaging protocols. Nonetheless, these structural insights help lay the foundation for understanding functional differences and should be complemented with functional imaging studies.

There are a few limitations to consider. The relatively small sample size was, in part, due to the 40-min acquisition time of the diffusion protocol with the available 3 T scanner. Lower functioning children were unable to complete the scan protocol and were thus under-represented in the current sample. New protocols with faster acquisition times will be integral to expanding the literature using NODDI methods with improved imaging protocols and technological advances such as multi-band/simultaneous multi slice imaging. In our protocol, one of the three collected diffusion datasets had a different TE and TR than the other two. As recommended, each shell was normalized by their $b = 0 \text{ s/mm}^2$ volume to attempt to minimize possible effects of differing acquisitions. Multi-shell datasets with matching acquisition parameters would be preferred. Another limitation was the loss to follow-up of the longitudinal cohort that has been followed since birth, due to loss of contact and attrition in participation. The original cohort was recruited during their stay in the neonatal intensive care unit six years prior to the current study.

Tract based spatial statistics also has its limitations. The FA skeleton only includes areas of highest FA within a tract to avoid voxels that contain partial volumes with other tissue such as grey matter and may not be representative of the entire white matter tract. In addition, the generation of the FA skeleton could be impacted by early white matter lesions. Another shortcoming of this method is its reliance on accurate registration between subjects. Multiple comparisons were taken into account using threshold-free cluster enhancement within analyses yet not across analyses, which should be taken into consideration when interpreting the results.

In conclusion, multi-shell diffusion imaging can assist in disentangling the microstructural properties in the white matter of children born very preterm. NODDI metrics of ODI and NDI have shown independent associations at the group level as well as with early brain injury and outcomes. In addition to DTI metrics, our findings support the use of NODDI metrics to provide more specific information of white matter microstructural differences that can improve detection and understanding of more slowly developing brain regions. In the children born very preterm, higher ODI in organized white matter regions such as the corpus callosum suggests disruption in white matter microstructure early in development. Associations between NDI and outcome measures in the very preterm children also suggest differing contributions of white matter microstructure to cognitive abilities compared to full-term children. Understanding the differences of white matter maturation at the microstructural level will increase our ability to identify biophysical elements of developmental processes that may be therapeutically targeted during the neonatal period in the future.

Acknowledgements

We thank all of the families who participated in the study. We also

thank Dr. Hilary Whyte, Dr. Charles Raybaud, Dr. Manohar Shroff, Tammy Rayner, Ruth Weiss, MyLoi Huynh-Silveira for their valuable support and contributions.

Funding source

Canadian Institutes of Health Research (MOP-84399 and MOP-137115).

Conflicts of interest

The authors have no conflicts of interest to declare.

Appendix A. Supplementary data

Supplementary data to this article can be found online at <https://doi.org/10.1016/j.nicl.2019.101855>.

References

- Anderson, M.J., Robinson, J., 2001. Permutation tests for linear models. *Australian New Zealand J. Stat.* 43 (1), 75–88. <https://doi.org/10.1111/1467-842X.00156>.
- Batalle, D., Hughes, E.J., Zhang, H., Tournier, J.-D., Tumor, N., Aljabar, P., ... Counsell, S.J., 2017. Early development of structural networks and the impact of prematurity on brain connectivity. *NeuroImage* 149, 379–392. <https://doi.org/10.1016/j.neuroimage.2017.01.065>.
- Beery, K., Buktenica, N., Beery, N., 2010. *Beery-Buktenica Test of Visual Motor Integration*. The Psychological Corporation, San Antonio, TX.
- Budde, M.D., Annese, J., 2013. Quantification of anisotropy and fiber orientation in human brain histological sections. *Front. Integr. Neurosci.* 7 (3). <https://doi.org/10.3389/fnint.2013.00003>.
- Carper, R.A., Treiber, J.M., White, N.S., Kohli, J.S., Müller, R.A., 2017. Restriction spectrum imaging as a potential measure of cortical neurite density in autism. *Front. Neurosci.* 10, 610. <https://doi.org/10.3389/fnins.2016.00610>.
- Catani, M., Howard, R.J., Pajevic, S., Jones, D.K., 2002. Virtual in vivo interactive dissection of white matter fasciculi in the human brain. *NeuroImage* 17 (1), 77–94. <https://doi.org/10.1006/nimg.2002.1136>.
- Chang, L.-C., Jones, D.K., Pierpaoli, C., 2005. RESTORE: robust estimation of tensors by outlier rejection. *Magn. Reson. Med.* 53 (5), 1088–1095. <https://doi.org/10.1002/mrm.20426>.
- Chang, Y.S., Owen, J.P., Pojman, N.J., Thieu, T., Bukshpun, P., Wakahiro, M.L.J., ... Mukherjee, P., 2015. White matter changes of neurite density and fiber orientation dispersion during human brain maturation. *PLoS One* 10 (6), e0123656. <https://doi.org/10.1371/journal.pone.0123656>.
- Counsell, S.J., Zhang, H., Hughes, E., Steele, H., Tumor, N., Ball, G., ... Edwards, D., 2014. In vivo assessment of neurite density in the preterm brain using diffusion magnetic resonance imaging. *Proc. Intl. Soc. Mag. Reson. Med.* 22.
- Dean, D.C., Planalp, E.M., Wooten, W., Adluru, N., Kecskemeti, S.R., Frye, C., ... Alexander, A.L., 2017. Mapping white matter microstructure in the one month human brain. *Sci. Rep.* 7 (1), 1–14. <https://doi.org/10.1038/s41598-017-09915-6>.
- Dubois, J., Dehaene-Lambertz, G., Perrin, M., Mangin, J.F., Cointepas, Y., Duchesnay, E., ... Hertz-Pannier, L., 2008. Asynchrony of the early maturation of white matter bundles in healthy infants: quantitative landmarks revealed noninvasively by diffusion tensor imaging. *Hum. Brain Mapp.* 29 (1), 14–27. <https://doi.org/10.1002/hbm.20363>.
- Duerden, E., Card, D., Lax, I.D., Donner, E.J., Taylor, M.J., 2013. Alterations in frontostriatal pathways in children born very preterm. *Dev. Med. Child Neurol.* 55 (10), 952–958. <https://doi.org/10.1111/dmnc.12198>.
- Eaton-rosen, Z., Melbourne, A., Orasanu, E., Cardoso, M.J., Modat, M., Bainbridge, A., ... Ourselin, S., 2015. Longitudinal measurement of the developing grey matter in preterm subjects using multi-modal MRI. *NeuroImage* 111, 580–589. <https://doi.org/10.1016/j.neuroimage.2015.02.010>.
- Genç, S., Malpas, C.B., Holland, S.K., Beare, R., Silk, T.J., 2017. Neurite density index is sensitive to age related differences in the developing brain. *NeuroImage* 148, 373–380. <https://doi.org/10.1016/j.neuroimage.2017.01.023>.
- Genç, S., Malpas, C.B., Ball, G., Silk, T.J., Seal, M.L., 2018. Age, sex, and puberty related development of the corpus callosum: a multi-technique diffusion MRI study. *Brain Struct. Funct.* 223 (6), 2753–2765. <https://doi.org/10.1007/s00429-018-1658-5>.
- Grussu, F., Schneider, T., Tur, C., Yates, R.L., Tachrount, M., Ianuş, A., ... Gandini Wheeler-Kingshott, C.A.M., 2017. Neurite dispersion: a new marker of multiple sclerosis spinal cord pathology? *Ann. Clin. Transl. Neurol.* 4 (9), 663–679. <https://doi.org/10.1002/acn3.445>.
- Jenkinson, M., Bannister, P., Brady, M., Smith, S., 2002. Improved optimization for the robust and accurate linear registration and motion correction of brain images improved optimization for the robust and accurate linear registration and motion correction of brain images. *NeuroImage* 17, 825–841. <https://doi.org/10.1006/nimg.2002.1132>.
- Jenkinson, M., Beckmann, C.F., Behrens, T.E.J., Woolrich, M.W., Smith, S.M., 2012. FSL. *NeuroImage* 62 (2), 782–790. <https://doi.org/10.1016/j.neuroimage.2011.09.015>.
- Jones, D.K., Knösche, T.R., Turner, R., 2013. White matter integrity, fiber count, and

- other fallacies: the do's and don'ts of diffusion MRI. *NeuroImage* 73, 239–254. <https://doi.org/10.1016/j.neuroimage.2012.06.081>.
- Kelly, C.E., Thompson, D.K., Chen, J., Leemans, A., Adamson, C.L., Inder, T.E., ... Anderson, P.J., 2016. Axon density and axon orientation dispersion in children born preterm. *Hum. Brain Mapp.* 37 (9), 3080–3102. <https://doi.org/10.1002/hbm.23227>.
- Kinney, H.C., Brody, B., Kloman, A., Gilles, F., 1988. Sequence of central nervous system myelination in human infancy. II patterns of myelination in autopsied infants. *J. Neuropathol. Exp. Neurol.* 47 (3), 217–234.
- Kostović, I., Judas, M., 2002. Correlation between the sequential ingrowth of afferents and transient patterns of cortical lamination in preterm infants. *Anat. Rec.* 267 (1), 1–6. <https://doi.org/10.1002/ar.10069>.
- Kunz, N., Zhang, H., Vasung, L., O'Brien, K.R., Assaf, Y., Lazeyras, F., ... Hüppi, P.S., 2014. Assessing white matter microstructure of the newborn with multi-shell diffusion MRI and biophysical compartment models. *NeuroImage* 96, 288–299. <https://doi.org/10.1016/j.neuroimage.2014.03.057>.
- Mah, A., Geeraert, B., Lebel, C., 2017. Detailing neuroanatomical development in late childhood and early adolescence using NODDI. *PLoS One* 12 (8), e0182340.
- Mangin, K.S., Horwood, L.J., Woodward, L.J., 2017. Cognitive development trajectories of very preterm and typically developing children. *Child Dev.* 88 (1), 282–298. <https://doi.org/10.1111/cdev.12585>.
- Melbourne, A., Eaton-Rosen, Z., Orasanu, E., Price, D., Bainbridge, A., Cardoso, M.J., ... Ourselin, S., 2016. Longitudinal development in the preterm thalamus and posterior white matter: MRI correlations between diffusion weighted imaging and T2 relaxation. *Hum. Brain Mapp.* 37 (7), 2479–2492. <https://doi.org/10.1002/hbm.23188>.
- Miller, S.P., Cozzio, C.C., Goldstein, R.B., Ferriero, D.M., Partridge, J.C., Vigneron, D.B., Barkovich, A.J., 2003. Comparing the diagnosis of white matter injury in premature newborns with serial MR imaging and transfontanel ultrasonography findings. *Am. J. Neuroradiol.* 24 (8), 1661–1669. Retrieved from. <http://www.ncbi.nlm.nih.gov/pubmed/13679289>.
- Mori, S., Wakana, S., Van Zijl, P.C.M., Nagai-Poetscher, L.M., 2005. *MRI Atlas of Human White Matter*. Elsevier, Amsterdam, The Netherlands.
- Nilsson, M., Lätt, J., Ståhlberg, F., van Westen, D., Hagslätt, H., 2012. The importance of axonal undulation in diffusion MR measurements: a Monte Carlo simulation study. *NMR Biomed.* 25 (5), 795–805. <https://doi.org/10.1002/nbm.1795>.
- Nossin-Manor, R., Card, D., Morris, D., Noormohamed, S., Shroff, M.M., Whyte, H.E.A., ... Sled, J.G., 2013. Quantitative MRI in the very preterm brain: assessing tissue organization and myelination using magnetization transfer, diffusion tensor and T1 imaging. *NeuroImage* 64, 505–516.
- Papile, L.A., Burstein, J., Burstein, R., Koffler, H., 1978. Incidence and evolution of subependymal and intraventricular hemorrhage: a study of infants with birth weights less than 1,500 gm. *J. Pediatr.* 92 (4), 529–534. [https://doi.org/10.1016/S0022-3476\(78\)80282-0](https://doi.org/10.1016/S0022-3476(78)80282-0).
- Rae, C.L., Davies, G., Garfinkel, S.N., Gabel, M.C., Dowell, N.G., Cercignani, M., ... Critchley, H.D., 2017. Deficits in neurite density underlie white matter structure abnormalities in first-episode psychosis. *Biol. Psychiatry* 82 (10), 716–725. <https://doi.org/10.1016/j.biopsych.2017.02.008>.
- Smith, S.M., Nichols, T.E., 2009. Threshold-free cluster enhancement: addressing problems of smoothing, threshold dependence and localisation in cluster inference. *NeuroImage* 44 (1), 83–98. <https://doi.org/10.1016/j.neuroimage.2008.03.061>.
- Smith, S.M., Jenkinson, M., Johansen-Berg, H., Rueckert, D., Nichols, T.E., Mackay, C.E., ... Behrens, T.E.J., 2006. Tract-based spatial statistics: Voxelwise analysis of multi-subject diffusion data. *NeuroImage* 31 (4), 1487–1505. <https://doi.org/10.1016/j.neuroimage.2006.02.024>.
- Tamnes, C.K., Roalf, D.R., Goddings, A.-L., Lebel, C., 2017. Diffusion MRI of white matter microstructure development in childhood and adolescence: methods, challenges and progress. *Dev. Cogn. Neurosci.* S1878-9293 (17). <https://doi.org/10.1016/j.dcn.2017.12.002>. 30008–7.
- Timmers, I., Roebroeck, A., Bastiani, M., Jansma, B., Rubio-Gozalbo, E., Zhang, H., 2016. Assessing microstructural substrates of white matter abnormalities: a comparative study using DTI and NODDI. *PLoS One* 11 (12), e0167884. <https://doi.org/10.1371/journal.pone.0167884>.
- Tusor, N., Benders, M.J., Counsell, S.J., Nongena, P., Ederies, M.A., Falconer, S., ... Edwards, A.D., 2017. Punctate White matter lesions associated with altered brain development and adverse motor outcome in preterm infants. *Sci. Rep.* 7 (1), 1–9. <https://doi.org/10.1038/s41598-017-13753-x>.
- Volpe, J.J., 2008. *Intracranial hemorrhage: Germinal matrix- intraventricular hemorrhage of the premature infant*. In: *Neurology of the Newborn, Fifth Edit.* Saunders, Philadelphia, USA, pp. 517–588.
- Wechsler, D., 1999. *Wechsler Abbreviated Scales of Intelligence (WASI)*. The Psychological Corporation, San Antonio, TX.
- Woodward, L.J., Moor, S., Hood, K.M., Champion, P.R., Foster-Cohen, S., Inder, T.E., Austin, N.C., 2009. Very preterm children show impairments across multiple neurodevelopmental domains by age 4 years. *Arch. Dis. Child. Fetal Neonatal Ed.* 94 (5), F339–F344. <https://doi.org/10.1136/adc.2008.146282>.
- Young, J.M., Morgan, B.R., Whyte, H.E.A., Lee, W., Smith, M., Lou, Raybaud, C., ... Taylor, M.J., 2017. Longitudinal study of White matter development and outcomes in children born very preterm. *Cereb. Cortex* 27 (8), 4094–4105. <https://doi.org/10.1093/cercor/bhw221>.
- Young, J., Vandewouw, M., Morgan, B., Smith, M., Sled, J., Taylor, M., 2018. Altered white matter development in children born very preterm. *Brain Struct. Funct.* 223 (5), 2129–2141. <https://doi.org/10.1007/s00429-018-1614-4>.
- Zhang, H., Schneider, T., Wheeler-Kingshott, C.A., Alexander, D.C., 2012. NODDI: practical in vivo neurite orientation dispersion and density imaging of the human brain. *NeuroImage* 61 (4), 1000–1016. <https://doi.org/10.1016/j.neuroimage.2012.03.072>.